REVIEW OF SCIENTIFIC INSTRUMENTS **77**, 043705 (2006)

Design of a femtosecond laser assisted tomographic atom probe

B. Gault, F. Vurpillot, A. Vella, M. Gilbert, A. Menand, D. Blavette, and B. Deconihout[a)]
GPM, UMR 6634 CNRS, Université et INSA de Rouen, 76801 Saint-Etienne du Rouvray Cedex, France

(Received 11 January 2006; accepted 14 March 2006; published online 10 April 2006)

A tomographic atom probe (TAP) in which the atoms are field evaporated by means of femtosecond laser pulses has been designed. It is shown that the field evaporation is assisted by the laser field enhanced by the subwavelength dimensions of the specimen without any significant heating of the specimen. In addition, as compared with the conventional TAP, due to the very short duration of laser pulses, no spread in the energy of emitted ions is observed, leading to a very high mass resolution in a straight TAP in a wide angle configuration. At last, laser pulses can be used to bring the intense electric field required for the field evaporation on poor conductive materials such as intrinsic Si at low temperature. In this article, the performance of the laser TAP is described and illustrated through the investigation of metals, oxides, and silicon materials. © *2006 American Institute of Physics.* [DOI: 10.1063/1.2194089]

I. INTRODUCTION

Over the last 15 years, the atom probe tomography (APT) or the three dimensional atom probe (3DAP) has undergone many improvements, making it a well established nanoanalysis tool in materials science.[1–3] Due to its ability to map out the distribution of single atoms in a material in the real space on a nearly atomic scale, it has been extensively applied to the investigation of a number of materials, allowing a better understanding of physical phenomena involved in materials science. At the time of the nanoelectronic and with the constant progresses made in the miniaturization of electronic devices, the TAP could be a key tool in the investigation of physical phenomena, such as dopant diffusion or interface segregation, that control the electrical properties of these devices.

In the conventional 3DAP, single atoms are field evaporated from the surface of a tiplike shape specimen biased at a high positive voltage. The use of high voltage (HV) pulses allows their chemical identification by time-of-flight mass spectrometry. However, in the case of poorly conductive materials, HV pulses cannot be properly transmitted to the specimen apex.[4] Due to the electrical environment surrounding the specimen, the system acts as a low pass filter with a cutoff frequency inversely proportional to the material resistivity. The resistivity over which a 3DAP analysis of a material is no longer possible depends on the instrument configuration. It can be estimated over $1-10^2\ \Omega$ cm.[5] A HV pulsed analysis of highly doped semiconductors with a resistivity of about $10^{-2}\ \Omega$ cm has recently been reported.[6] In addition to make the TAP analysis of poor conductive materials impossible, the need for HV pulses results in two other drawbacks of the technique. The use of HV pulses with a duration in the nanosecond range results in a spread in the energy of emitted ions. The resulting spread in ion flight times makes the mass resolution of the technique insufficient. It has been shown that the use of an energy compensating device, such as a reflectron lens, can significantly improve the mass resolution.[7,8] However, these devices have a limited acceptance angle so that they cannot be used in a 3DAP with a significantly enlarged field of view. Lastly, sample rupture is often observed under HV pulsing probably due to the cycling stress generated by the pulses during the analysis.[9] This is particularly the case in the investigation of oxides or multilayers deposited on a metal or semiconductor substrate. Due to their poor adherence on the substrate, these layers are often observed to be removed at once as soon as HV pulses are applied on the specimen.

Over the last 30 years, different attempts have been made in order to overcome these atom probe drawbacks. The main concern was to extend the field of application of the technique to poor conductive materials. In addition, efforts have been made in order to significantly increase the amount of data resulting from a sample investigation by increasing the field of view of the technique.

A first approach to overcome these shortcomings is the scanning atom probe (SAP) introduced by Nishikawa and Kimofo in 1993.[10] In the SAP, a large number of tips are prepared onto a flat substrate. A single tip can be selected by means of a microelectrode (ME) accurately positioned a few microns above the tip. Atoms are removed from the surface of the tip by means of high voltage pulses and projected onto a position-sensitive detector (PSD) in the same way as in a conventional 3DAP. In the SAP, the small amount of data that results from the analysis of a single tip is counterbalanced by the large number of tips available. The most innovative idea in the SAP is that, because the tip to ME distance is small, lower voltages are required to reach the evaporation field of the material. By using a dual electrode, a postacceleration and/or a postdeceleration of ions may be used to lower the relative energy spread of emitted ions, resulting in an improved mass resolution.[11,12] Despite the significant increase in mass resolution, it is still insufficient to clearly resolve the mass peaks of chemical elements with very close

[a)]Electronic mail: bernard.deconihout@univ-rouen.fr

 © 2006 American Institute of Physics

Downloaded 14 Apr 2006 to 193.52.145.138. Redistribution subject to AIP license or copyright, see http://rsi.aip.org/rsi/copyright.jsp

mass to charge ratio.[13,14] However, the SAP meets with technical problems due to the small distance between the ME and the specimen array. Because the ME is placed very close to the sample which is positively biased, any asperity on the ME can act like a microtip negatively biased so that a field emission can occur, leading to the possible destruction of the ME. At the end, since the SAP still relies on HV pulsing assisted field evaporation, its application to insulating materials encounters the same issues as those encountered in the conventional 3DAP. However, it is worth noting that significant progresses have been made in the SAP development and have provided interesting results, in particular, in the investigation of highly doped semiconductor materials.[6,15]

In the 1980's Tsong and co-workers designed the pulsed laser atom probe (PLAP) in which HV pulses were replaced by nanosecond laser pulses.[4,16–18] These works were made on the former one-dimensional atom probe[19] that only differs from the 3DAP by a much smaller field of view since no position-sensitive detector is used. It was shown that the use of laser pulsing offers several advantages as compared with HV pulsing. First, the investigation of poor conductive materials was then possible. A number of works dedicated to the investigation of semiconductor materials,[20–22] ceramics,[23] or oxide layers could be conducted for the first time. Another advantage of laser pulsing is the absence of significant ion energy spread, resulting in a high mass resolution. Mass resolution over 4000 full width at half maximum (FWHM) was reported,[18] allowing the design of a straight atom probe with a high mass resolution.

In the PLAP, because the duration of laser pulses was in the nanosecond or subnanosecond range, the field evaporation of atoms was thermally assisted. The tip apex was heated up to temperatures allowing a thermal promotion of the field evaporation process. The calculations of Liu and Tsong[24] show that the peak temperature of the specimen under nenosecond laser pulse illumination can reach 500 K for the highest laser powers. However, Tsong showed that the evaporation was possible with a limited temperature increase by using small thermal pulse amplitude.[25,26] In order to avoid preferential evaporation of low evaporation field species, a sufficiently high power density was required. This was achieved by a strong focusing onto the tip apex. Such a focusing is difficult to achieve in a reproductive manner, making the amount of energy deposited on the specimen difficult to control. As a result, the optimum conditions giving reliable composition measurements were sometimes very difficult to achieve.[22] These technical difficulties are probably the reasons why no laser 3DAP has been implemented since the emergence of the 3DAP in the 1990s. Some authors suggested the use of shorter pulses to avoid some of the thermal pulsing drawbacks.[27] Shorter laser pulses lead to a higher laser intensity, making the focusing procedure easier. They also mentioned a possible role of the laser field itself in the field evaporation of ions, even if the effective process evoked then was still the thermal activation of field evaporation.

In 2004, we proposed to use femtosecond laser pulses to field evaporate the materials in the 3DAP.[28,29] Because the electron-phonon coupling time is of a few tens of picoseconds at low temperatures,[30] ultrafast laser pulses (100 fs) should avoid any significant heating of the specimen during the pulse. In addition, works made in the scanning near-field optical microscopy domain for instance, have shown that when a tiplike shape specimen with subwavelength dimensions is illuminated by femtosecond laser pulses, the laser field is strongly enhanced by large surface plasmon oscillations.[31–33] We have shown that, due to the field enhancement, the laser field can be very intense, over a few V/Å, typical value required for field evaporation.[29] In this article, the design of a femtosecond laser assisted TAP is presented and its general performance is discussed and illustrated through the investigation of metals and semiconductors.

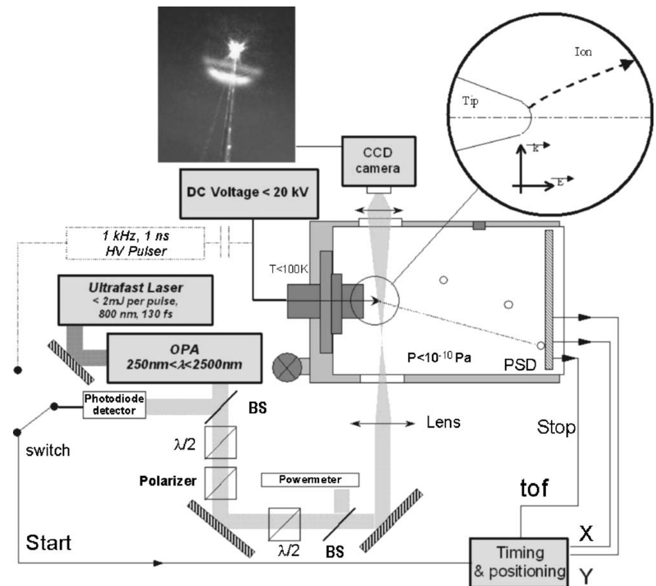

FIG. 1. Experimental setup scheme.

II. INSTRUMENT DESIGN

The laser TAP is basically a conventional TAP in which an ultrafast laser has been incorporated (Fig. 1). The instrument can be used either in the conventional pulsed voltage (PV) mode or in the pulsed laser (PL) mode. The position-sensitive detector used in this study is a delay line detector with improved multihit capabilities.[34] It consists of a conventional 4.3 cm Roentdek delay line detector following a pair of microchannel plates (MCPs) in a chevron configuration. Signal output from each end of the two wire pairs are digitized by means of fast digitizer boards (PXI DC 271 Acquiris). The real time sampling of signals is made at 1 or 4 gigasamples (GS)/s with a bandwidth of 1 GHz. Ion flight time signals are taken as output from the MCP, and the positioning is calculated using signals provided by the delay line outputs. A deconvolution algorithm is used to improve the multihit capabilities of PSD. During this work the PSD could be placed either at 58 cm (conventional configuration) or at 19 cm in a wide angle (WA) configuration.

The laser system is a chirped pulse amplified Ti:Sa femtosecond laser (Quantronix Integra-I). with an average power of up to 2 W at 1 kHz. The pulse length is 120 fs at a wavelength of 788 nm. It is constituted by a doped fiber femto-

Downloaded 14 Apr 2006 to 193.52.145.138. Redistribution subject to AIP license or copyright, see http://rsi.aip.org/rsi/copyright.jsp

second oscillator. The pulse is amplified using two Ti:Sa stages. The output beam is a TEM_{00} Gaussian beam with a diameter of 8 mm. The laser beam is sent into the analysis chamber through a glass window. The laser power can be tuned from 0 to 2 W using an attenuator stage. The linear polarization can also be rotated by means of a zero-order half-wave plate. The beam is focused by a lens of focal length of 25 cm. The actual size of the spot onto the specimen cannot be measured. It is estimated from the equation of propagation of a Gaussian beam focused by a lens. The lens position is set for its focal point to be in the UHV to avoid either air ionization at the focal point or damage of the glass window. Furthermore a charge coupled device (CCD) camera (AVT Marlin F-046B) placed above the tip gives a magnified image of the tip with a precision of about 10 μm. A beam shutter is also available to work in PVAP. A fast photodiode (EOT) is used to accurately measure the moment at which a laser pulse is sent onto the tip. This signal is used to trig the time of flight measurement channel. In order to ensure a good stability of the laser power, the whole electronic device is synchronized on the 1 kHz internal clock of the laser that delivers pulses at 1 kHz. At last, an optical parametric amplifier (Light Conversion, TOPAS 4/800) has been recently implemented at the output of the laser to enable to tune the wavelength from 275 to 2200 nm.

III. RESULTS

A. Laser assisted field evaporation

In the 3D atom probe, surface atoms are removed by the application of a high electric field F. This field is obtained by applying a voltage V on the tip of radius R:

$$F = \frac{V}{\beta R}, \tag{1}$$

where β is a geometric factor.[35,36]

The presence of F at the surface makes ionic states more stable than atomic states as the distance from the surface increases. Ionization is possible because of thermal vibrations that allow atoms to overcome the surface potential barrier. The probability P to field evaporate an atom follows a Maxwell-Boltzmann law, $P = \nu \exp - Q(F)/k_B T$, with ν the atom vibration frequency, $Q(F)$ the field-dependent potential barrier, k_B the Boltzmann constant, and T the tip temperature. P is thus very sensitive to the field F and can be accurately adjusted via the total field set around a value called the threshold evaporation field (TEF).

In the HV pulsed atom probe, a fraction (typically 20%) of the total voltage V is applied by means of HV pulses that lowers the potential barrier height for a short time (1 ns), allowing the chemical identification of the evaporated ions by time of flight mass spectrometry. For a flight path L, assuming that an ion of mass over charge ratio M acquires the whole energy on a very short distance, the mass is given by

$$M = K(V_{dc} + V_p)\frac{t^2}{L^2}, \tag{2}$$

where t is the ion flight time, K a constant, V_{dc} the standing voltage, and V_p the pulse amplitude. In order to avoid the preferential evaporation of atoms having the lowest evaporation field, the pulse fraction $\alpha = V_p/(V_{dc}+V_p)$ has to be set at a minimum value that ranges from 15% to 25% depending on the material to be analyzed. Due to Eq. (1), α is also the fraction of the pulsed field F_p over the total field applied on the specimen, $\alpha = F_p/(F_{dc}+F_p)$.

In the field evaporation assisted by laser pulses, a standing field is applied on the specimen by means of a standing voltage V_{dc} while the pulsed field is generated by the laser itself. For a laser with a pulse energy E_p and a duration τ focused on a spot of diameter D, the intrinsic laser field F_i can be calculated from the formula linking the peak intensity I and the Poynting vector of the plane wave produced by the laser source:

$$I = \frac{4E_p}{\pi D^2 \tau} = \frac{\epsilon_0 c}{2} F_i^2, \tag{3}$$

with ϵ_0 the electric permittivity of the vacuum and c the celerity of light in vacuum. At optical frequencies (10^{15} Hz), the laser field oscillates too fast to allow the field evaporation of surface atoms. The potential barrier is lowered during a time much smaller that the vibration time of surface atoms (10^{-13} s). We have recently shown that the field evaporation process under femtosecond laser pulsing cannot be explained by a thermal process nor by a photon excitation mechanism as proposed by Tsong in the case of nanosecond laser pulses.[25] We have shown that the laser field generates a terahertz pulse at the tip surface with a duration equal to the duration of the laser pulse, τ, sufficient to promote the field evaporation of surface atoms.[37] The generation of this terahertz pulse involves a nonlinear optical process called optical rectification that is only possible at the specimen surface constituting a lack of symmetry in the material. In addition the optical rectification signal is enhanced due to the laser field enhancement at the surface. The amplitude of this terahertz pulse depends on many parameters such as the dielectric permittivity of the medium, the laser intensity or the wavelength, and the polarization of the wave. A good estimate of this amplitude can be obtained from Ref. 37 where it is shown that the actual field brought by the wave is much higher than the intrinsic laser field F_i. The ratio between the laser field F_{laser} and the intensity I is an important parameter hereafter called the laser field factor (LFF) ℓ.

In the laser assisted (LA) field evaporation, ℓ has to be determined in order to set the fraction of the pulsed field α at a value close to that commonly used in the HV mode. There are different ways to determine ℓ. A first method is based on the observation of the field evaporation of a material in the field ion microscope (FIM). In the FIM, the surface of the specimen can be imaged with an atomic resolution. An imaging gas (usually He or Ne) is introduced in the UHV chamber while a high voltage is applied to the specimen. Due to the high electric field at the tip surface, gas atoms are field-ionized and projected onto an imaging screen where they

Downloaded 14 Apr 2006 to 193.52.145.138. Redistribution subject to AIP license or copyright, see http://rsi.aip.org/rsi/copyright.jsp

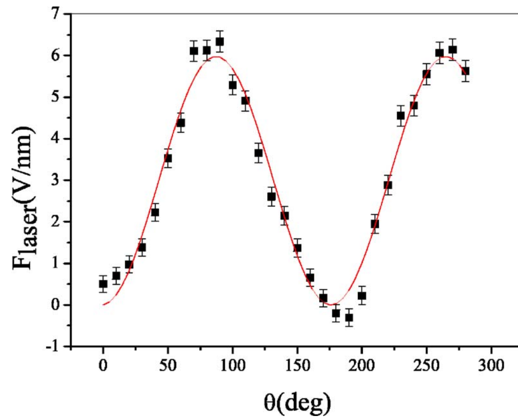

FIG. 2. Effective laser field as a function of the angle of polarization of the wave with respect to the main tip axis.

form an image of the surface with a high magnification. If the specimen voltage is increased further, the surface field is sufficient to promote the field evaporation of the material. Thus, by comparing the standing voltage necessary to reach the TEF in the HV mode and that necessary to obtain the evaporation under laser illumination, a measurement of F_{laser} can be made. The dependence of F_{laser} on the angle of polarization of the wave as observed on a pure W specimen is reported in Fig. 2. The W was imaged in He so that the TEF of W is $F_{\text{th}} \approx 50$ V nm^{-1}. The pulse energy and the spot diameter were set in order to get an energy density of 40 μJ mm^{-2}. For an axial polarization, the standing voltage required to remove W atoms was about 8 kV, corresponding to a standing field $F_{\text{dc}} \approx 43$ V nm^{-1}. As a result, the effective laser field is 7 V nm^{-1} and $\ell \approx 0.2$ V nm^{-1}/GW cm^{-2}. Note that the effective laser field is 70 times larger than the intrinsic laser field F_i that can be estimated to 0.1 V nm^{-1}. The effective laser field can also be simply measured in the 3DAP analysis mode by performing an analysis in HV mode prior to the LA mode. The comparison of the total voltage required to remove the material in HV mode and the standing voltage required in LA mode gives a good estimate of the actual laser field. Note that this procedure has only to be done once on a material. The ℓ factor depends on the material and can vary from an order of magnitude from one material to another. However, it has been shown[37] that the effective laser field (ELF) dependence on θ follows a square cosine law for all materials:

$$F_{\text{laser}} = \ell I \cos^2 \theta. \tag{4}$$

This dependence is shown in Fig. 2. This makes it possible to control the ELF applied on the specimen by tuning the polarization of the wave by means of a second zero-order half-wave plate (Fig. 1).

A sequence of the field evaporation of W atoms on a (110) W pole under laser illumination is shown in Fig. 3. The evaporation is very steady and the way the material is removed looks very similar to what is observed in the HV mode. Kink site atoms located on the pole edges are first removed so that the pole radius smoothly decreases until it is reduced to a single atom. Neither atom migration prior to the evaporation nor promotion of atoms from deeper layers has been observed conversely to observations made under nanosecond laser pulse illumination.[16] This suggests a small temperature increase under pulsed laser illumination during and after the pulses. This has been confirmed by our recent study of the tip temperature evolution after the application of a femtosecond laser pulse. These results are described elsewhere.[38] They showed that the tip temperature increase was below 200 K for W and below 50 K for Al, temperatures far too low to allow a thermally activated field evaporation. A temperature of at least 350 K would have been required in the case of W. In addition, the temperature was found to drop down to the specimen average temperature ($\approx$50 K) in a few hundred nanoseconds, i.e., in a time much smaller than the millisecond that separates two successive laser pulses.

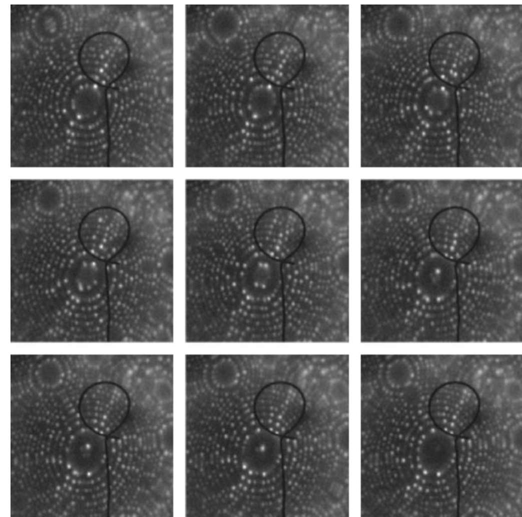

FIG. 3. FIM image showing the evaporation sequence of the (110) pole on a pure W specimen illuminated by femtosecond laser pulses (tip temperature of 40 K, 10^{-5} mbar of He, 40 μJ/pulse).

B. Time-of-flight mass spectrometry

The alignment of the beam on the tip is made by means of a CCD camera focused on the specimen. The beam is roughly positioned on the shank of the tip using the micrometer screws of the lens and the mirror. The spot is then moved along the main tip axis so as to observe a diffraction pattern indicating that the spot is located at the tip apex (picture in Fig. 3). Note that due to the field enhancement, a strong focusing is not necessary and the spot diameter is set around 1 mm. This makes the alignment very easy and ensures that the tip apex is located is the beam, even in case of possible vibrations of the specimen generated by the cooling stage for instance.

The ELF is set at about 20% of the TEF and the dc voltage is then increased until the evaporation of atoms is detected. In order to compensate for the tip radius increase due to the removal of the material, the dc voltage is continuously increased in the same way as in the HV mode. The laser field can also be increased to keep the pulse fraction sufficient by rotating the polarization of the wave. However, while in the case of the conventional 3DAP the pulse fraction has to be kept constant over the whole analysis, an accurate knowledge of the laser field amplitude is not necessary to

Downloaded 14 Apr 2006 to 193.52.145.138. Redistribution subject to AIP license or copyright, see http://rsi.aip.org/rsi/copyright.jsp

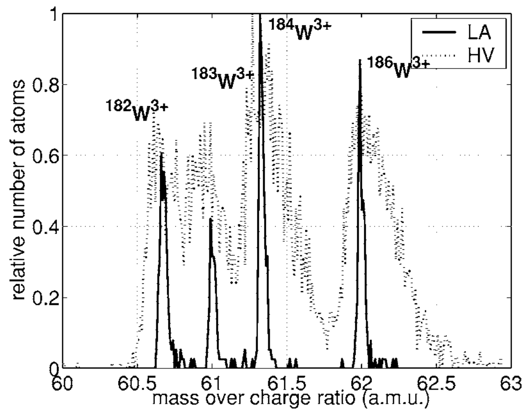

FIG. 4. W^{3+} mass peaks as measured from a LA TAP analysis (black) and a HV TAP analysis of a pure W specimen.

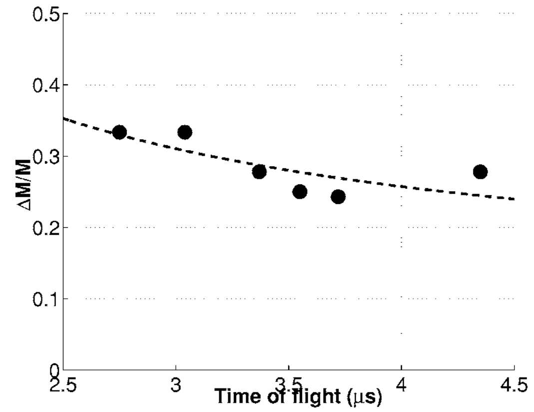

FIG. 5. Mass resolution changes as a function of the flight time of ions. The observed values are compared with the values expected from Eq. (6) (solid line) with a timing accuracy of 0.8 ns.

calculate the mass over charge ratio M of ions. M is found to depend only on the standing voltage applied to the specimen:

$$M = KV_{\mathrm{dc}}\frac{t^2}{L^2}. \tag{5}$$

Because of the very short duration of the evaporation pulse (terahertz), ions are accelerated by the standing voltage only. A mass spectrum obtained from the LA TAP analysis of a pure W specimen is given in Fig. 4. As it can be seen, peaks related to different W^{3+} isotopes are detected with the right mass over charge ratio using Eq. (5). This mass spectrum is compared with that obtained in the conventional HV mode in the same conditions. The mass resolution improvement is clear, all the W^{3+} isotope peaks being well separated conversely to the HV mode. In addition, in the LA mode mass peaks do not have the exponentiallike shape tail having a quasi-Gaussian shape. The mass resolution is 1500 FWHM and 750 full width tenth of the maximum (FWTM) in the laser mode. In the HV mode, it is only 250 FWHM and about 50 FHTM. This suggests the absence of a significant energy spread of the emitted ions as expected from the very short duration of the pulse. Ions are mainly accelerated by the dc field in the same way as in the former PLAP. The mass resolution results from errors made on the measurements of the flight time, the flight path, and the voltage applied on the specimen, V_{dc}. From Eq. (5) we can write

$$\left(\frac{\Delta M}{M}\right)^2 = \left(\frac{\Delta V_{\mathrm{dc}}}{V_{\mathrm{dc}}}\right)^2 + \left(2\frac{\Delta t}{t}\right)^2 + \left(2\frac{\Delta L}{L}\right)^2. \tag{6}$$

The error on the distance simply generates a systematic shift of the mass spectrum that can be easily corrected. Note that this is true only if the detector is small enough or position sensitive. The standing voltage is measured by means of a 16 bit analog-to-digital converter. The error made on the total voltage is then $\Delta V_{\mathrm{dc}}/V_{\mathrm{dc}} \approx 5.10^{-5}$ for the worst case.[14] Timing errors are controlled by the precision of the PSD used in this study. For a sampling frequency of 1 GHz, it can be estimated below 1 ns.[34] As the voltage on the specimen increases, flight times decrease so that the relative timing error varies with V_{dc}. The changes of $\Delta M/M$ with the flight times are reported in Fig. 5. The evolution expected from Eq. (6) with a timing error of 0.8 ns (dashed line) is consistent with the experimental points.

C. 3D imaging capabilities

In the 3DAP, ions removed from the specimen surface are projected onto a position-sensitive detector. The magnification of a 3DAP is $G=L/(m+1)R$ with m a constant close to 1. For a typical tip radius R of 50 nm and a flight path $L=0.5$ m, G is close to 10^7. Atom position within the surface of analysis is simply the impact coordinates onto the PSD divided by G. 3D images are reconstructed assuming that all the atoms occupy the same volume in the material. For each detected atom, the depth in the 3D image is increased from the same amount.[2] During an analysis, due to the material removal, the tip radius continuously increases and the magnification changes. In the HV mode, the change in R is compensated by an increase of the total voltage so as to keep the surface electric field equal to the evaporation field F of the material. The change of the tip radius, and hence the change of the magnification, is simply derived from the measurement of the applied voltage,

$$G = \frac{L}{(m+1)R} = \frac{LF\beta}{(m+1)(V_{\mathrm{dc}}+V_p)}. \tag{7}$$

In the LA TAP, the electric field applied on the specimen can be much larger than the evaporation field of the material. In addition, only a good estimate of the actual terahertz pulse amplitude can be obtained so that the magnification is more difficult to determine. The simplest way to determine the evolution of G during the analysis is to perform a short analysis in the HV mode prior to the LA investigation. The starting tip radius is then determined and, assuming that the tip has a constant shank angle, the change in R and thus in G can be simply related to the amount of material collected along the analysis.

A 3D image obtained from the analysis of an Al based alloy is shown in Fig. 6. The reconstruction was made assuming a constant shank angle of 3°. Al (100) planes are well resolved in a direction close to the direction of analysis. This is confirmed by the diffraction pattern as obtained from the Fourier transform made on the 3DAP data set. This ability to

Downloaded 14 Apr 2006 to 193.52.145.138. Redistribution subject to AIP license or copyright, see http://rsi.aip.org/rsi/copyright.jsp

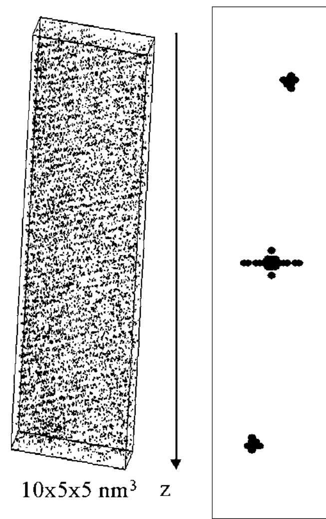

FIG. 6. (Left) 3D image resulting from the LA TAP analysis of an aluminum based alloy showing Al atomic planes. (Right) 3D diffraction pattern showing that Al (100) planes are resolved.

resolve atomic planes has been observed on a wide variety of materials. This confirms that the field evaporation process in LA mode and in HV mode are very similar. This also validates the simple reconstruction procedure used to map out the atom distribution in the 3D images. As it can be seen in Fig. 6, the Al plan spacing remains constant and equal to 0.2 nm over the whole analysis volume. Note that the assumption of a constant shank angle is often valid but not always, since the tip shape can change from one sample to another. More refined procedures will have to be developed. A possible way to determine G would be to derive the amplitude of the laser field from the evaporation rate and from the value of the standing voltage using Eq. (1).

The LA TAP has been applied on a wide variety of materials in order to demonstrate its ability to give quantitative 3D images resolved at the atomic scale. We first investigated well known materials whose chemical properties have already been obtained from conventional TAP investigations. As an example, the composition measurement as obtained from the analysis of a SC16 Ni based superalloy are reported in Table I. This material contains large aluminum enriched precipitates. Measured concentrations are in good agreement with those resulting from the conventional TAP investigation. This ability to give reliable composition measurements has been verified on all sorts of materials. This demonstrates that no preferential evaporation of the species having the lowest evaporation field occurred during the analysis. This has been possible because of the estimation of the effective

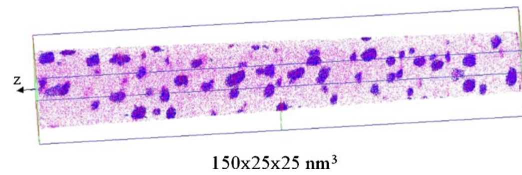

FIG. 7. LA TAP analysis of FeCuTi alloys in a semi-WA configuration. The size of the volume is $25 \times 25 \times 150$ nm^3. Only Cu atoms are represented.

laser field that makes possible to set the pulsed field fraction over 20% on all types of materials.

The new ability to obtain a good mass resolution in a straight-type 3DAP configuration makes possible to enlarge the field by placing the position-sensitive detector closer to the specimen.[28] Of course, because flight times are shortened, relative errors on timing are larger and the mass resolution expected in a wide angle configuration would be less than that observed with a conventional field of view. Analyses have been performed with a flight path of 19 cm, i.e., in a semi-WA configuration. Figure 7 gives a 3D image obtained from the LA investigation of an FeCuTi alloy. Due to the larger field of view, the number of Cu precipitates intercepted is much larger than in the conventional TAP, making the determination of the volume fraction of precipitates or their composition measurement easier and more reliable.

D. Investigation of poorly conductive materials

As previously mentioned, the laser TAP has been used to investigate a wide variety of materials. It has been found that specimens are much less sensitive to rupture than in the HV mode. This could be explained by the duration of the terahertz pulses which is too short to excite phonon lattice. As a result, no cycling stress is applied to the specimen, avoiding a fatigue induced rupture. Of course this remains to be demonstrated by dedicated investigations. Many types of materials whose analysis could never be done in the conventional TAP could be analyzed in the laser TAP. For instance, oxide layers developed on metal tips[39] or multilayers deposited on silicon substrates could successfully be characterized. These results will be detailed in a dedicated paper.

Si specimen could also be investigated with the laser TAP. In the HV TAP, the nanosecond pulses cannot be properly transmitted to the tip apex on resistive materials. Due to the sample resistance, the HV pulse is broadened, making the time of flight analysis difficult and causing the material to be removed by clusters or in the form of complex molecular ions. This is illustrated in Fig. 8 which shows showing a mass spectrum related to the conventional TAP analysis of a

TABLE I. Comparison of concentrations measured with the conventional TAP and with the LA TAP in a Ni based superalloy.

Element	Al (%)	Ti (%)	Cr (%)	Fe (%)	Ni (%)	Mo (%)	Ta (%)
HV TAP	12.04	7.92	1.73	0.02	75.59	0.53	2.18
	±0.16	±0.13	±0.06	±0.01	±0.21	±0.04	±0.07
LA TAP	12.43	8.08	2.06	2.07	75.18	0.84	1.34
	±0.33	±0.27	±0.14	±0.03	±0.43	±0.09	±0.11

Downloaded 14 Apr 2006 to 193.52.145.138. Redistribution subject to AIP license or copyright, see http://rsi.aip.org/rsi/copyright.jsp

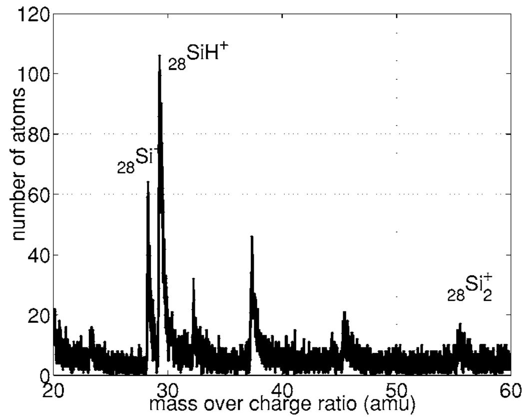

FIG. 8. HV TAP mass spectrum obtained from the analysis of a low B doped silicon sample at 70 K (material resistivity $\approx 1\ \Omega$ cm.

low B doped Si with an electrical resistivity slightly over 1 Ω cm. Many molecular species such as silicon hydrides or silicon clusters are detected. Due to the enlargement of the evaporation pulse, mass peaks present a wide tail lying on several amu, making the identification of the different chemical species difficult. We have investigated an intrinsic Si sample with a high purity (impurity level $\approx 10^{11}$ cm^{-3}). The tip was prepared by ion milling using a focused ion beam[40] with a Ga ion source. The mass spectrum obtained with the laser TAP and the resulting 3D image are shown in Fig. 9. As it can be seen Si is mainly field evaporated as single ions despite the detection of a small fraction of Si clusters. Mass peaks are well defined and no molecular ions were formed during the evaporation. This demonstrates that the pulsed field is efficiently applied at the specimen surface. The specimen resistivity being above $10^4\ \Omega$ cm at room temperature and the tip temperature being 40 K during the analysis, this specimen can be considered as an insulator since no carriers can be excited at such a low temperature. One can note in the mass spectrum small peaks related to the detection of Ga ions at the beginning of the analysis. These ions come from the milling process during which Ga ions are implanted in the vicinity of the specimen surface on a distance that can be estimated to 2 nm from the 3D image provided in Fig 9.

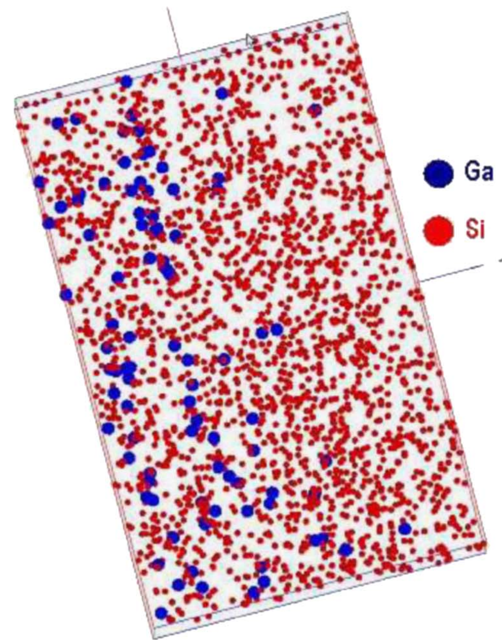

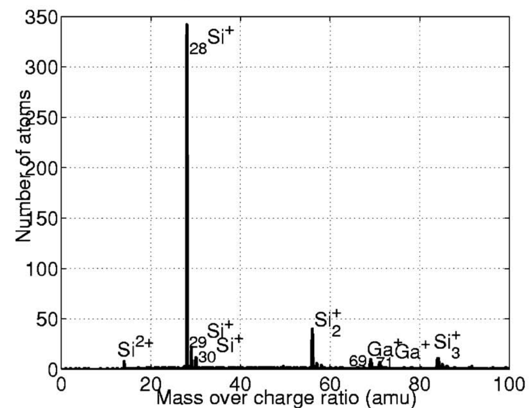

FIG. 9. Laser TAP mass spectrum and 3D image obtained from the analysis of an intrinsic silicon sample at 40 K (material resistivity $\approx 10^4\ \Omega$ cm.). The size of the image is $5 \times 3 \times 3$ nm^3. Ga atoms are imaged in the first layers of the sample.

IV. DISCUSSION

Results presented in this work show that the use of ultrafast laser pulses makes possible to design a 3DAP with improved performances as compared with the conventional 3DAP. The field evaporation is assisted by the ultrafast pulsed field generated by the laser on the specimen whose duration is below 1 ps as described in Ref. 37. This weakens the energy spread of the emitted ions, resulting in a significant improvement of the mass resolution. The observed mass resolution can be better than $\Delta M/M = 1000$, i.e., even larger than that of conventional 3DAP equipped with an energy compensating device. Because these devices have an acceptance angle limited to about 10°, it was not possible to enlarge the field of view of the technique. The new ability to get a high mass resolution in a straight-type configuration makes possible to fully open the field of view so as collect the whole amount of material available from the specimen.

As mentioned in the Introduction, one of the main advantages of the field evaporation lies in its surface nature allowing an in-depth investigation of a material with a resolution equal to an atomic layer. We have shown that atomic planes can be resolved in the LA TAP. This can be explained by the surface nature of the optical rectification process responsible for the terahertz pulse generation. Because the surface constitutes a lack of symmetry in the material, the laser induced electric field lies near the surface of the sample, preserving the unique in-depth spatial resolution of the 3DAP.

The ability to field evaporate poor conductive materials such as intrinsic Si was already demonstrated in the 1980s when the former pulsed laser atom probe was developed. However, at that time, the field evaporation was assisted by the thermal pulse induced by a strong photon absorption. In the LA TAP, the field evaporation process is different and the tip temperature increase under laser illumination has been found to be much too small to allow a thermally activated process. This temperature increase is clearly also too low to promote atom diffusion prior to evaporation that would lead

Downloaded 14 Apr 2006 to 193.52.145.138. Redistribution subject to AIP license or copyright, see http://rsi.aip.org/rsi/copyright.jsp

to a loss in the spatial resolution. Due to the subwavelength dimensions of the specimen apex, the laser field is strongly enhanced so that typical intense evaporation fields can easily be achieved without a need of a strong focusing of the light onto the specimen. Laser pulses of a few tenths of a microjoules focused on about 0.5–1 mm have found to be sufficient to probe a wide variety of materials. This ensures an easy alignment procedure together with a good immunity to mechanical vibrations always possible in this type of sophisticated instrument.

Electric fields much larger than the threshold evaporation field of the material can be applied conversely to the conventional 3DAP in which the application of large evaporation pulses leads to a systematic tip rupture. This brings a decisive advantage over the conventional TAP since very fragile materials can be investigated by keeping the dc field sufficiently low to avoid the specimen rupture.

All our experimental results have been obtained at a wavelength of 780 nm. This wavelength is far from typical wavelengths necessary to generate plasmon resonance in a material and hence a resonant enhancement of the field. This can explain why no significant difference in the behavior of materials under laser illumination is observed. It is clear that the LA field evaporation will have to be investigated at other wavelengths. An optical parametric amplifier has recently been incorporated allowing to tune the wavelength from 275 to 2200 nm. The use of UV pulses seems interesting, in particular, in the investigation of insulator materials in which the break of strong covalent bounds is required. However, at such wavelengths, the LA field evaporation might be induced by a strong photon absorption of the medium so that a larger specimen temperature increase can be expected. In addition, the field enhancement should be quite different because of possible plasmon resonance. We plan to investigate all these effects in the near future.

ACKNOWLEDGMENTS

The authors thanks F. de Geuser and E. Cadel for the specimen preparation. This work has been supported by the CNRS (DAE, SPM, and STIC departments), the French Ministry of Research and Technology, and the Fond National pour la Science (nanoscience program).

[1] D. Blavette, A. Bostel, J. Sarrau, B. Deconihout, and A. Menand, Nature (London) **363**, 432 (1993).
[2] D. Blavette, B. Deconihout, A. Bostel, J. M. Sarrau, M. Bouet, and A. Menand, Rev. Sci. Instrum. **64**, 2911 (1993).
[3] A. Cerezo, T. J. Godfrey, and G. D. W. Smith, Rev. Sci. Instrum. **59**, 862 (1988).
[4] T. Tsong, S. McLane, and T. Kinkus, Rev. Sci. Instrum. **53**, 1442 (1982).
[5] A. J. Melmed, M. Martinka, S. M. Girvin, T. Sakurai, and Y. Kuk, Appl. Phys. Lett. **39**, 416 (1981).
[6] K. Thompson, J. H. Booske, D. J. Larson, and T. F. Kelly, Appl. Phys. Lett. **87**, 052108 (2005).
[7] A. Cerezo, T. J. Godfrey, S. J. Sijbrandij, G. D. W. Smith, and P. J. Warren, Rev. Sci. Instrum. **69**, 49 (1998).
[8] E. Bémont, A. Bostel, M. Bouet, G. Da Costa, S. Chambreland, B. Deconihout, and K. Hono, Ultramicroscopy **95**, 231 (2003).
[9] K. Hono (private communication).
[10] O. Nishikawa and M. Kimoto, Appl. Surf. Sci. **77**, 424 (1994).
[11] S. S. Bajikar, D. J. Larson, T. F. Kelly, and P. P. Camus, Ultramicroscopy **65**, 119 (1996).
[12] M. Huang, A. Cerezo, P. Clifton, and G. Smith, Ultramicroscopy **89**, 163 (2001).
[13] A. Cerezo, T. J. Godfrey, M. Huang, and G. D. W. Smith, Rev. Sci. Instrum. **71**, 3016 (2000).
[14] B. Deconihout, R. Saint-Martin, C. Jarnot, and A. Bostel, Ultramicroscopy **95**, 239–249 (2003).
[15] T. F. Kelly and D. J. Larson, Mater. Charact. **44**, 59 (2000).
[16] G. Kellogg and T. Tsong, J. Appl. Phys. **51**, 1184 (1980).
[17] T. Tsong, J. Phys. F: Met. Phys. **8**, 1349 (1978).
[18] T. Tsong, Y. Liou, and S. McLane, Rev. Sci. Instrum. **55**, 1246 (1984).
[19] E. W. Müeller, J. A. Panitz, and S. B. McLane, Rev. Sci. Instrum. **39**, 83 (1968).
[20] A. Cerezo, C. Grovenor, and G. Smith, J. Microsc. **141**, 155 (1986).
[21] Y. Hasegawa, T. Hashizume, T. Sakurai, and Y. Mizushima, J. de Physique, supplment au n°11, 47 (1986).
[22] T. Hashizume, Y. Hasegawa, A. Kobayashi, and T. Sakurai, Rev. Sci. Instrum. **57**, 1378 (1986).
[23] M. Miller, P. Angelini, A. Cerezo, and K. More, Colloq. Phys. **50**, 459 (1989).
[24] H. F. Liu and T. T. Tsong, Rev. Sci. Instrum. **55**, 1779 (1974).
[25] T. Tsong, Phys. Rev. B **30**, 4946 (1984).
[26] T. Tsong, Surf. Sci. **177**, 594 (1986).
[27] M. Miller, A. Cerezo, M. Hetherington, and G. Smith, *Atom Probe Field Ion Microscopy* (Clarendon, Oxford, 1996).
[28] B. Deconihout, F. Vurpillot, B. Gault, A. Hideur, M. Brunel, A. Bostel, M. Bouet, G. da Costa, A. Menand, and D. Blavette, Surf. Interface Anal. (to be published).
[29] B. Gault, F. Vurpillot, A. Bostel, A. Menand, and B. Deconihout, Appl. Phys. Lett. **86**, 094101 (2005).
[30] D. von der Linde, K. Sokolowski-Tinten, and J. Bialkowski, Appl. Surf. Sci. **109**, 1 (1997).
[31] L. Novotny, R. X. Bian, and X. S. Xie, Phys. Rev. Lett. **79**, 645 (1997).
[32] O. J. F. Martin and C. Girard, Appl. Phys. Lett. **70**, 705 (1997).
[33] Y. C. Martin, H. F. Hamann, and H. K. Wickramasinghea, J. Appl. Phys. **89**, 5774 (2001).
[34] G. D. Costa, F. Vurpillot, A. Bostel, M. Bouet, and B. Deconihout, Rev. Sci. Instrum. **76**, 013304 (2005).
[35] E. Mueller, Phys. Rev. **103**, 618 (1956).
[36] R. Gomer, J. Chem. Phys. **13**, 341 (1959).
[37] A. Vella, F. Vurpillot, B. Gault, A. Menand, and B. Deconihout, Phys. Rev. B (submitted).
[38] F. Vurpillot, B. Gault, A. Vella, M. Bouet, and B. Deconihout, Appl. Phys. Lett. **88**, 094105 (2006).
[39] B. Gault, A. Menand, F. de Geuser, B. Deconihout, and R. Danoix, Appl. Phys. Lett. **88**, 114101 (2006).
[40] D. Larson, D. Foord, A. Petford-Long, A. Cerezo, and G. D. W. Smith, Nanotechnology **10**, 45 (1999).

Downloaded 14 Apr 2006 to 193.52.145.138. Redistribution subject to AIP license or copyright, see http://rsi.aip.org/rsi/copyright.jsp